Protein Science (1999), *8*:410–417. Cambridge University Press. Printed in the USA.

Breaking the low barrier hydrogen bond in a serine protease

RICHARD D. KIDD,[1] PAMELA SEARS,[2] DEE-HUA HUANG,[2] KRISTA WITTE,[2] CHI-HUEY WONG,[2] AND GREGORY K. FARBER[1]

[1]Department of Biochemistry and Molecular Biology, The Pennsylvania State University, 108 Althouse Laboratory, University Park, Pennsylvania 16802

[2]Department of Chemistry and Skaggs Institute for Chemical Biology, The Scripps Research Institute, 10550 North Torrey Pines Road, La Jolla, California 92037

Abstract

The serine protease subtilisin BPN′ is a useful catalyst for peptide synthesis when dissolved in high concentrations of a water-miscible organic co-solvent such as N,N-dimethylformamide (DMF). However, in 50% DMF, the k_{cat} for amide hydrolysis is two orders of magnitude lower than in aqueous solution. Surprisingly, the k_{cat} for ester hydrolysis is unchanged in 50% DMF. To explain this alteration in activity, the structure of subtilisin 8397+1 was determined in 20, 35, and 50% (v/v) DMF to 1.8 Å resolution. In 50% DMF, the imidazole ring of His64, the central residue of the catalytic triad, has rotated approximately 180° around the Cβ-Cγ bond. Two new water molecules in the active site stabilize the rotated conformation. This rotation places His64 in an unfavorable geometry to interact with the other members of the catalytic triad, Ser221 and Asp32. NMR experiments confirm that the characteristic resonance due to the low barrier hydrogen bond between the His64 and Asp32 is absent in 50% DMF. These experiments provide a clear structural basis for the change in activity of serine proteases in organic co-solvents.

Keywords: conformational change; organic co-solvents; protein crystallography; subtilisin

Currently, there is significant interest in the behavior of enzymes dissolved or suspended in water with a high concentration of a water miscible organic co-solvent. In the presence of an organic co-solvent, enzymes can catalyze reactions that are thermodynamically or kinetically impossible in water (Zaks & Klibanov, 1985; Kuhl et al., 1990; Stahl et al., 1990; West et al., 1990) and can use molecules that would not be substrates in water (Homandberg et al., 1978; Zaks & Klibanov, 1986, 1988; Gololobov et al., 1992; Tawaki & Klibanov, 1992). These changes in activity are particularly interesting for serine proteases. The serine proteases show decreased amide hydrolysis in co-solvents while their ester hydrolysis activity changes little. Since both amide and ester hydrolysis reactions proceed through the same chemical mechanism, it is surprising that the two reactions would show such different dependence on changes in the solvent. In addition, it has been shown that the ability of subtilisin to catalyze peptide synthesis is increased in the presence of organic co-solvents to a degree that is difficult to explain based on the decrease in water concentration alone (Sears et al., 1994). To explain these observations, we have used protein crystallography and NMR spectroscopy to examine the structure of the active site of subtilisin in the presence and absence of an organic co-solvent.

Subtilisin BPN′ (EC 3.4.21.14), a serine protease from *Bacillus amyloliquefaciens*, has been used as a catalyst for large-scale peptide synthesis (Wong, 1989; Abrahmsen et al., 1991). The use of a serine protease for peptide synthesis reduces the need for protecting groups and nearly eliminates the problem of racemization during standard solid-phase peptide syntheses (Wells & Estell, 1988). DMF is an ideal solvent because it both solubilizes substrates and shifts the equilibrium away from proteolysis and toward peptide synthesis by reducing the availability of water and suppressing the ionization of the amine nucleophile and the charged groups resulting from the hydrolysis (Sears et al., 1994).

Unfortunately, wild-type subtilisin is not stable in the concentrations of DMF necessary for peptide synthesis (Zhong et al., 1991a). Site-directed mutagenesis was used to create a series of subtilisin mutants, which solved this stability problem in DMF (Pantoliano et al., 1989; Wong et al., 1990; Zhong et al., 1991a; Sears et al., 1994) . We have solved the structure of one of these mutants, subtilisin 8397+1 (Kidd et al., 1996). This structure showed that the basis for increased stability is due to the enhanced binding of a calcium ion. Although subtilisin has been engineered to inactivate more slowly than the wild-type enzyme, its maximal activity toward amide substrates is much lower in high concentrations of DMF than in water; k_{cat} for amide hydrolysis is reduced by two orders of magnitude (Wong et al., 1990).

Reprint requests to: Gregory K. Farber, The Pennsylvania State University, Department of Biochemistry/Molecular Biology, 108 Althouse Laboratory, University Park, Pennsylvania 16802-4500; e-mail: farber@ewald.bmb.psu.edu.

Table 1. *Data collection and reduction statistics*

	Native	20% DMF	35% DMF	50% DMF
Unit cell dimensions[a]				
a	41.56 ± 0.01	41.57 ± 0.04	41.67 ± 0.08	41.57 ± 0.06
b	79.53 ± 0.04	79.67 ± 0.02	79.62 ± 0.04	79.70 ± 0.07
c	37.25 ± 0.02	37.22 ± 0.02	37.23 ± 0.02	37.18 ± 0.06
β	114.48 ± 0.04	114.13 ± 0.04	114.27 ± 0.04	114.24 ± 0.08
Reflections collected	21,228	21,228	21,228	21,228
Reflections observed ($>2\sigma$)	14,501	15,425	10,660	10,322
Resolution (Å)	1.8	1.8	1.8	1.8
Crystals	4	3	3	3
R-merge[b] (%)	11.3	6.2	7.3	8.2
Isomorphous difference[c] (%)				
20% DMF	8.7			
35% DMF	15.6	12.8		
50% DMF	15.8	16.8	5.2	

[a]Errors are the standard deviation of the mean of all crystals.
[b]*R*-merge is $\Sigma|I_j - I_{ave}|/\Sigma I_{ave}$ where *j* is a summation over all crystals.
[c]The isomorphous difference is $\Sigma|F_{\text{lower DMF}} - F_{\text{higher DMF}}|\Sigma F_{\text{lower DMF}}$ DMF with the summation taken over all common reflections.

Clearly, a structural study of this mutant in both environments is necessary to explain the changes in activity. Here we report the refined crystal structures of subtilisin 8397+1 at 1.8 Å in an aqueous mother liquor and in mixtures of this mother liquor with DMF. These structures show that the lower activity in DMF is due to a conformational change involving the active site histidine. Data collection and data refinement statistics for the structures are listed in Tables 1 and 2.

Results and discussion

Changes in structure due to DMF

In general, DMF has had little effect on the backbone and side-chain conformations between the four structures. The overall RMS deviation between the native and 50% DMF structures is 0.53 Å.

Table 2. *Refinement statistics*

	Native	20% DMF	35% DMF	50% DMF
Water molecules[a]	90	65	147	229
Calcium ions	2	2	2	2
R-factor (%)	18.5	21.5	17.7	18.7
Bond lengths[b]	0.012	0.010	0.011	0.012
Bond angles[b]	1.694	1.663	1.713	1.728
Mean *B*-factor (Å^2)				
Main chain	18.94	14.01	2.61	4.57
Side chain	21.69	15.69	3.36	6.21
Overall protein	20.13	14.74	2.93	5.28
Waters	33.83	27.85	19.29	17.31
A-site calcium	20.57	20.40	2.01	5.20
B-site calcium	38.83	23.65	7.54	28.87
PDB code	1SBH	1YJA	1YJB	1YJC

[a]There are 1,943 nonhydrogen atoms in each of the structures. No DMF molecules were detected in any of the electron density maps.
[b]RMS deviations from ideal values.

In the active site, the structures are very similar except in 50% DMF (Fig. 1). As is expected for a serine protease, His64 interacts with the other members of the catalytic triad, Asp32 and Ser221. The hydrogen bond between Asp32 and His64 is particularly short (2.65 Å) and has been described as a low-barrier hydrogen bond in a number of serine proteases (Markley, 1978; Frey et al., 1994; Tobin et al., 1995), although this description is not universally accepted (Ash et al., 1997). The strong interaction between Asp32 and His64 is responsible for shifting the Nδ1-H resonance of His64 very far downfield in the NMR spectrum (Markley, 1978; Frey et al., 1994; Tobin et al., 1995; Halkides et al., 1996).

When the catalytic triad of subtilisin 8397+1 in 50% DMF was first examined, there was a noticeable rotation of the histidine imidazole ring relative to the native structure. Initially, it appeared that the ring of the 50% structure had rotated approximately 16°; however, the imidazole had also swung away from the side chain of Asp32, lengthening the low barrier-hydrogen bond to normal hydrogen bond length. In addition to this movement away from the Asp32 side chain, two new ordered water molecules have appeared near the His imidazole in the 50% DMF structure (Fig. 1B).

Since the critical Asp-His low barrier-hydrogen bond was different in the 50% DMF structure, a closer examination of all of the key bonds in the active site was warranted. A total of five subtilisin structures were compared (Fig. 1A). In these structures, the average bond length between the Asp32 side-chain oxygen and the His64 Nδ is 2.65 ± 0.04 Å. In contrast, this hydrogen bond length is 2.86 Å for 8397+1 in 50% DMF (Fig. 1B). Two other conserved hydrogen bond distances also show significant changes in the catalytic site of the 50% DMF structure. The Asp Oδ2 to Ser33 N distance, which averages 2.76 ± 0.03 Å for the five subtilisin structures (Fig. 1A), has decreased to 2.64 Å in the 50% structure. This motion causes the distance from a conserved water to the Asp Oδ1 to increase from 2.66 ± 0.04 Å to 2.91 Å.

From the change in hydrogen bond lengths shown in Figure 1, it appears that the imidazole ring of His64 in the 50% structure may not have rotated 16° as originally thought, but approximately 164°. A reexamination of the $2F_o - F_c$ maps (Fig. 2) and simulated annealing omit-maps (Fig. 3) was undertaken to help determine if

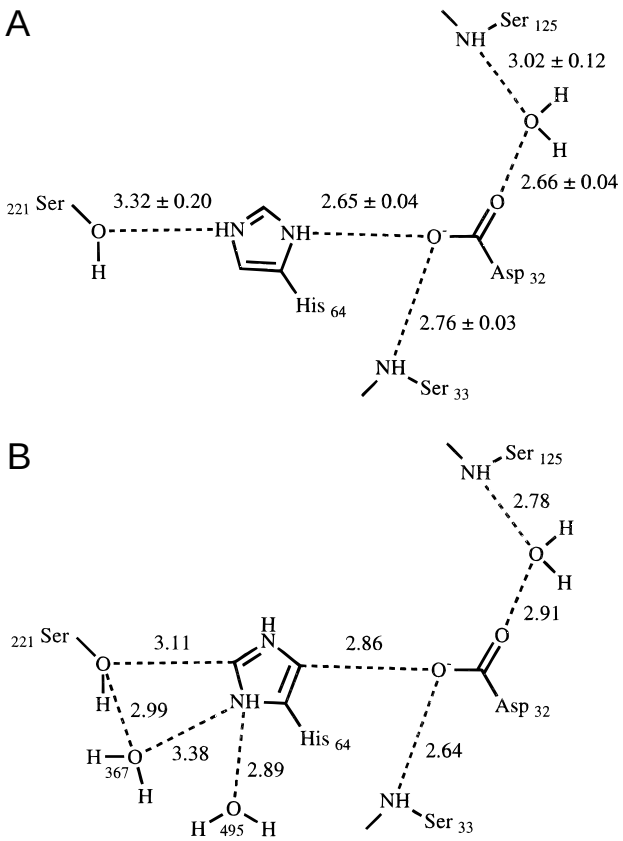

Fig. 1. Schematic diagram of the distances (in angstroms) between residues of the catalytic triad (Ser221, His64, and Asp32). **A:** Mean and standard deviations of hydrogen bond distances for the crystallographic model subtilisin 8350 (PDB code 1S01) (Pantoliano et al., 1989), subtilisin 8397 (PDB code 1SBI) (Wong et al., 1990), and subtilisin 8397+1 in 0, 20, and 35% dimethylformamide (DMF). The short hydrogen bond distance between the His64 and Asp32 side chains is conserved among serine proteases. Nϵ of His64 is the proximal nitrogen to Oγ of Ser221 and Nδ is the proximal nitrogen to the Asp32 side chain. Both His64 nitrogens are shown protonated in this figure because the crystals were grown below the pK_a of His Nϵ (p$K_a \approx 7$) (Bachovchin & Roberts, 1978). **B:** Distances between water molecules and residues in part of the active site of subtilisin 8397+1 in 50% DMF. The His64 imidazole is displayed with a conformation that shows the ring rotated ~180° around the bond between the His64 Cβ and Cγ atoms relative to the other three structures. In the 50% DMF structure, there are two additional water molecules near His64.

this ring-flip had actually occurred in the 50% DMF structure. It is difficult to distinguish nitrogens from carbons at 1.8 Å resolution; however, there is a definite bulge in the density for the Nδ in Fig. 3B (50%) compared to the density of Cδ in Fig. 3A (native). In addition, the slight bulge in density for the Nϵ atom in the 0, 20, and 35% structures is not present in Fig. 3B. Instead, a slight bulge (above the plane of the ring) is present at the new Nϵ position in the 50% structure. These maps suggest that the increased electron density for the nitrogen is due to a flip of the imidazole ring.

NMR experiments confirm the conformational change in 50% DMF

If the side chain of His64 has flipped in 50% DMF, then the hydrogen bond between Asp32 and His64 should be broken since the atom facing the oxygen of the Asp is now a carbon rather than a nitrogen. The loss of this interaction should cause the signal for His64 to shift upfield in a proton NMR spectrum. The position of this peak in the NMR spectrum is dependent on the protonation state of His64 (Halkides et al., 1996). In the imidazolium form, the Nδ1-H proton peak appears at approximately 18 ppm, while in the imidazole form the peak shifts to 15 ppm (Halkides et al., 1996). Both positions are substantially downfield from the other histidine protons in serine proteases, which typically have resonances between 10–12 ppm (Ash et al., 1997). To keep the enzyme in the fully protonated state, one can either acidify the solution or to add a transition state analog such as trifluoromethylketone (Halkides et al., 1996). We conducted experiments under both conditions, with subtilisin 8397+1 dissolved in either a low pH pyridinium-HCl buffer (pH 5) or a higher pH Tris-HCl buffer (pH 7.5) with 5 mM Boc-Ala-Val-Phe-trifluoromethylketone, a known transition state analog of subtilisin.

The spectra recorded from the low pH studies are shown in Figure 4A. Both the imidazole (15 ppm) and the imidazolium (17.4 ppm) Nδ1-H peaks are visible, indicating that the histidine is partially deprotonated at this pH. The peaks are broad, and the imidazolium is a bit more upfield than expected, perhaps due to rapid exchange between the two states. Neither peak is visible in the spectrum of subtilisin 8397+1 with 50% DMF added. The peak is also greatly reduced in the presence of the trifluoromethylketone inhibitor in DMF (Fig. 4B).

Thermodynamics of the low-barrier hydrogen bond

Both the crystallographic results and NMR spectrum are consistent with a flipped conformation for His64 in 50% DMF. Two questions remain: what stabilizes this altered conformation, and does this altered conformation explain why subtilisin is less active toward amide substrates in DMF while the rate of the reaction with ester substrates is unchanged?

It seems strange that the charged side chain of His64 would flip away from Asp32 in 50% DMF since electrostatic interactions are expected to be stronger as the polarity of the solvent decreases. At the pH of the crystal structure and NMR experiments, we expect that both His64 and Asp32 are charged. It is possible that Asp32 becomes protonated in 50% DMF, but this seems an unlikely explanation for the His ring flip since the pK_a of the catalytic aspartic acid in serine proteases is unusually acidic (Markley & Ibañez, 1978). In chymotrypsin, this pK_a is below 2 (Fersht & Renard, 1974). The close similarity of the overall structure of subtilisin in 50% DMF to that in an aqueous solution also argues against a dramatic shift in the pK_a of Asp32. A more reasonable explanation involves the changes in the solvent structure observed only in the 50% DMF structure.

Two new water molecules are observed in the active site of the 50% DMF structure (Fig. 2). These water molecules form hydrogen bonds with the Nδ of catalytic histidine imidazole in the flipped conformation. None of the hydrogen bonds formed by these waters is nearly as short as the His-Asp bond in the native structure, although a new short bond has formed between the Od2 of Asp32 and the backbone nitrogen of Ser33. There are several ways to explain the thermodynamics of this structure. It is possible that the new 2.64 Å bond between Asp32 and Ser33 (Fig. 1B) is also a low barrier hydrogen bond, which is energetically equivalent to the bond between His64 and Asp32 in the native structure. It is also possible that the free energy of the low barrier hydrogen bond in

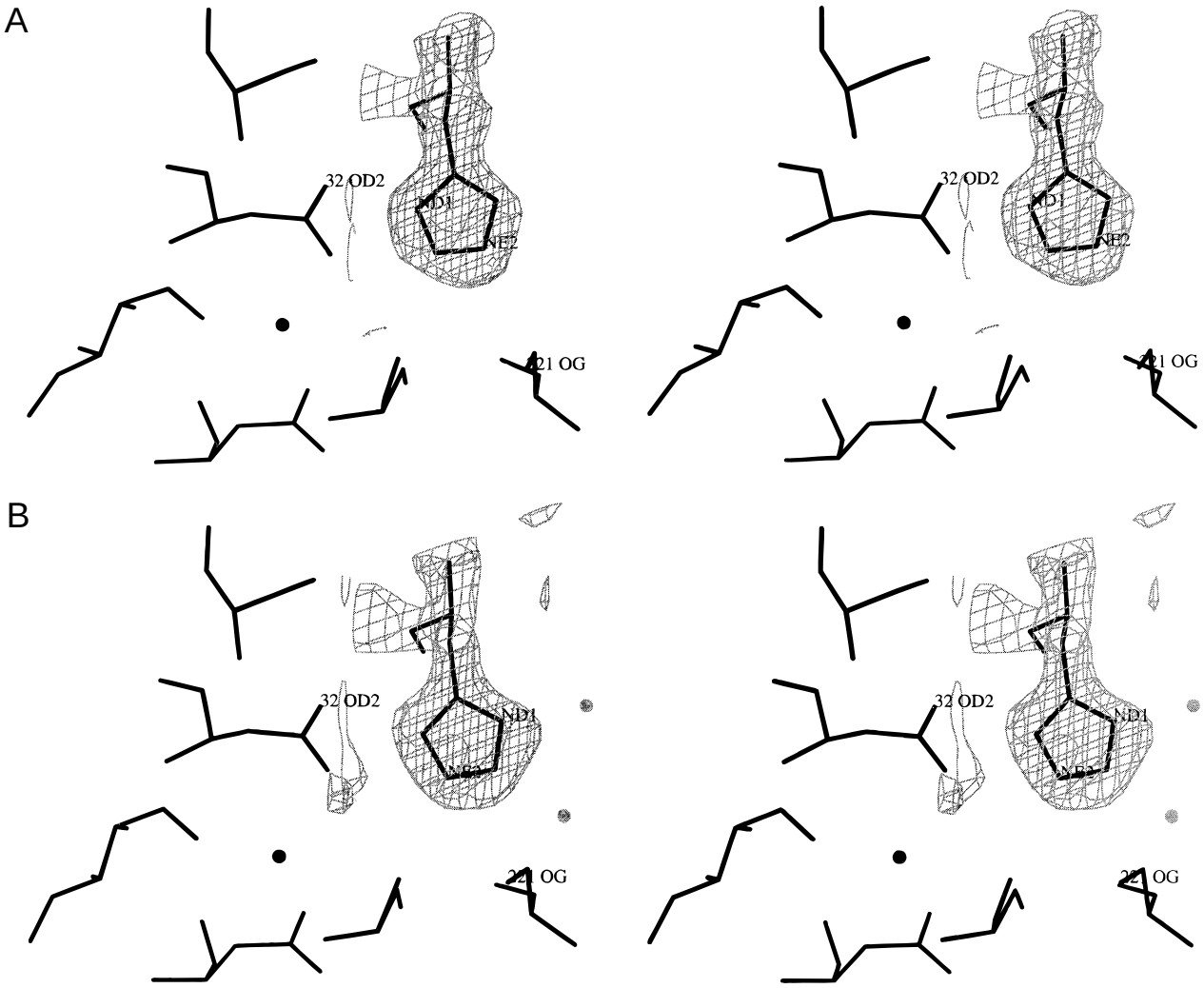

Fig. 2. Stereoview of part of the active site of subtilisin 8397+1 with electron density maps of catalytic histidine 64. **A:** Native structure. **B:** 50% DMF structure. The F_c and phases of the $2F_o - F_c$ map (contoured at 1.2σ) were derived from the protein model. Oδ2 of catalytic Asp32, Nδ and Nϵ of catalytic His64, and Oγ of catalytic Ser221 are labeled in both panels. The conserved water molecule (black circle) and the residues that tightly surround it are shown below Asp32. Two new water molecules that interact with the His64 imidazole are shown in **B**. This figure was generated with the program O (Jones et al., 1991).

the native structure is replaced by the two new hydrogen bonds in the active site in 50% DMF minus the cost of immobilizing two new waters. It is not easy to quantitate the free energy associated with this second scenario due to the perturbations caused by DMF in both hydrogen bond strength and in the entropy of immobilizing a water molecule.

Changes in enzyme activity

The conformational change between the catalytic His and Ser presents an explanation for the observed decrease in catalytic activity in DMF. In order for the enzyme to catalyze substrate hydrolysis, the histidine either flips back to the original conformation or uses the ϵ nitrogen as a general base without stabilization by the active site aspartic acid residue. The ϵ nitrogen is a much more likely general base than the δ nitrogen due to the distance to Ser221. Using His64 as the general base without stabilization from Asp32 is similar to the mechanism proposed for the modified serine proteases methylsubtilisin (Zhong et al., 1991b) and methylchymotrypsin (Wong et al., 1990). In these enzymes, the histidine is methylated at the ϵ nitrogen. It has been suggested that the presence of the methyl group forces the ring to flip, so that the δ nitrogen becomes the catalytic base, and thus the protonated imidazole lacks stabilization by the catalytic aspartic acid residue (Henderson, 1971; Byers & Koshland, 1978). Methylsubtilisin displays a large drop in amidase activity (nearly a 500-fold drop in k_{cat}) but only a small drop in esterase activity (5-fold drop in k_{cat}) (Zhong et al., 1991b). This decrease is similar in magnitude to that observed for subtilisin dissolved in high concentrations of organic co-solvent. In contrast to these cases where methylation causes the loss in stabilization by Asp32, in DMF the altered conformation is stabilized by the new solvent structure in the active site.

The results presented in this paper clearly show the structural basis for the observed decrease in amide hydrolysis of subtilisin in the presence of high concentrations of an organic co-solvent. The analysis shows that the solvent structure can be as important for

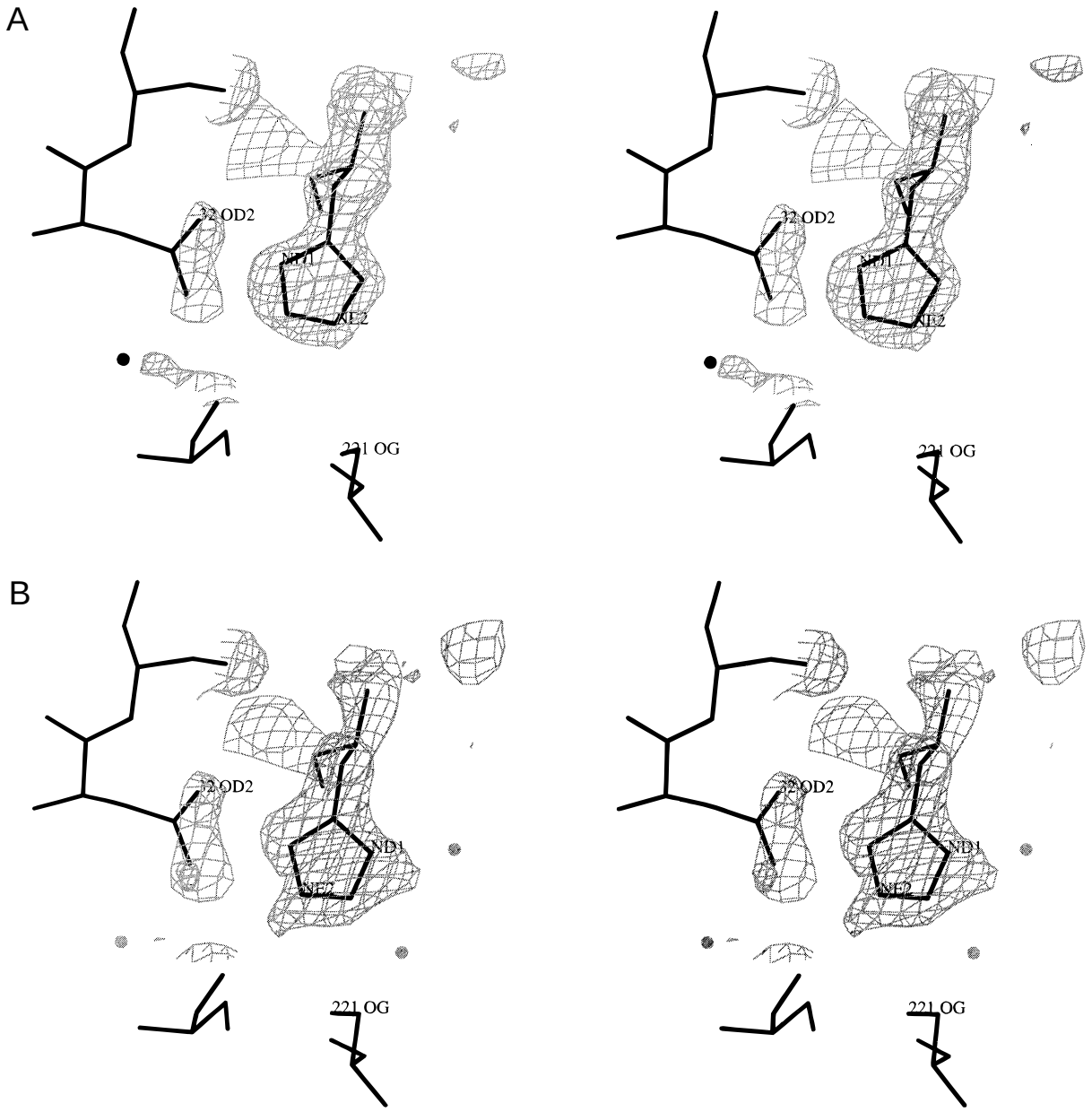

Fig. 3. Simulated annealing omit maps of catalytic histidine 64 of subtilisin 8397+1 in (**A**) 0% and (**B**) 50% dimethylformamide. For both panels, the density comes from a $2F_o - F_c$ map with F_c and phases derived from the model with omitted residues in a 5 Å sphere centered around Cγ of His64. Atoms in a 3 Å shell from 5 to 8 Å were harmonically restrained to prevent them from migrating into the omitted sphere. The contour level for both maps is 1.0σ. The density in both panels is overlaid against the unaltered models. Nδ and Nϵ of His64 are labeled in both panels.

activity as the protein structure. These results also show that the techniques used to understand structure/function relationships of enzymes in aqueous solvents can, with care, be used to understand the unusual changes in reactivity displayed by enzymes in organic co-solvents.

Materials and methods

Protein purification

Site-directed mutagenesis of 8397 to produce 8397+1 was performed as previously described (Kidd et al., 1996). The 8397+1 variant contained the following amino acid substitutions compared to the wild-type protein (Pantoliano et al., 1989; Kidd et al., 1996): K256Y, N218S, Q206C, G169A, N76D, and M50F. The purification of subtilisin 8397+1 was a modification of the procedure of Carter and Wells (1987), and it has been described elsewhere (Sears et al., 1994; Kidd et al., 1996).

Crystal growth

Subtilisin 8397+1 was crystallized by hanging drop vapor diffusion. The protein drop contained 5–10 mg/mL protein, 5 mM sodium cacodylate, 8.5% (w/v) PEG 3400, 8.5% (v/v) 2-propanol,

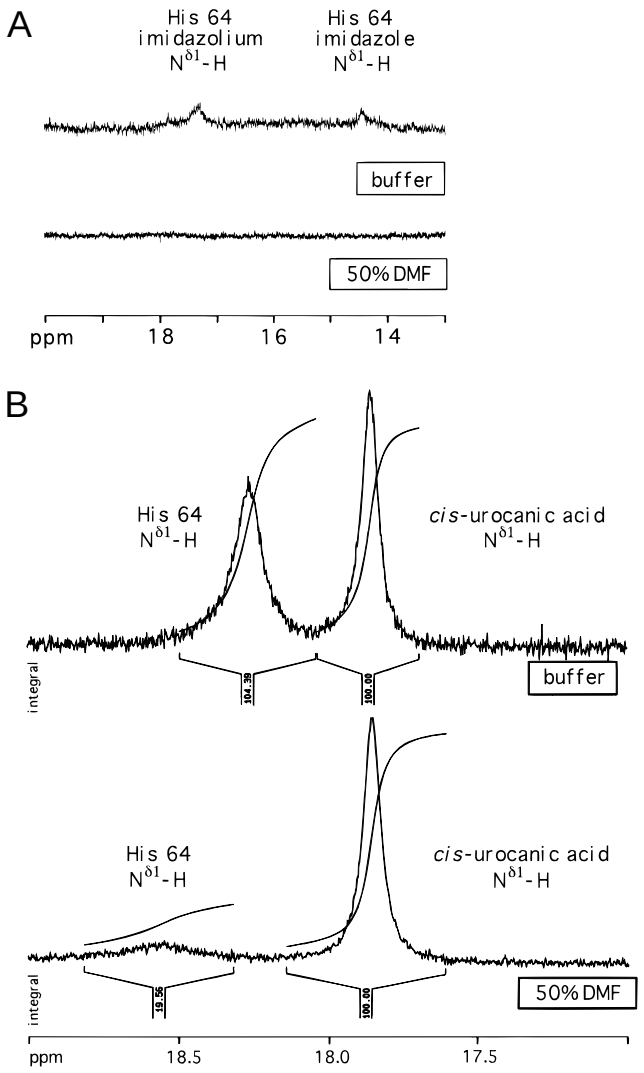

Fig. 4. NMR spectra which confirm the ring flip of His64 in 50% DMF. **A:** The spectrum recorded at low pH. Both the imidazole (15 ppm) and the imidazolium (17.4 ppm) Nδ1-H peaks are visible indicating that the histidine is partially deprotonated at this pH. The peaks are broad, and the imidazolium is a bit more upfield than expected, perhaps due to rapid exchange between the two states. Neither peak is visible in the spectrum of subtilisin with 50% DMF added. **B:** The spectrum recorded in the presence of a transition state analog. Only the imidazolium Nδ1-H peak is observable at 18.3 ppm. An external standard known to have a strong downfield absorbance, cis-urocanic acid (Ash et al., 1997) was included in the sample to allow a quantitative comparison of the two spectra. Removal of the standard (spectra not shown) verified that no peaks were hidden beneath the *cis*-urocanic acid peak. In the sample containing 50% DMF, the area of the Nδ1-H peak diminished to less than 20% of the peak area in the buffer, and the small remaining peak was shifted slightly downfield to approximately 18.55 ppm. No peak was observed near 15 ppm in the DMF sample indicating that DMF did not simply cause the histidine to deprotonate.

50 mM sodium citrate (pH 5.6). This drop was equilibrated against a reservoir containing 17% (w/v) PEG 3400, 17% (v/v) 2-propanol, 100 mM sodium citrate (pH 5.6). The initial volume of the protein drop was 20 μL and the volume of the reservoir was 1 mL. These crystals usually took 20 days to reach full size.

Crystal soaks in DMF

To determine the maximum amount of DMF that the crystals would tolerate while still showing reasonable diffraction, a flow cell was constructed as previously described (Petsko, 1985). A large crystal of 8397+1 was placed inside a capillary tube and wedged in place by pipe cleaner fibers. A reservoir for the soak solutions was attached to the capillary tube via Intramedic polyethylene tubing (Becton-Dickinson, Parsippany, New Jersey) that had been sealed to the capillary tube with sticky wax. A waste reservoir was attached in the same manner and positioned below the level of the soak reservoir. The flow cell assembly was mounted on a precession camera. Soak solutions were flowed over the crystal in 10% increments of DMF every two days. Approximately 20 mL of solution went through the flow cell in 24 h. After each increase in DMF concentration, the system was allowed to equilibrate for 24 h and then a 60 min X-ray still photo was taken of the crystal. These experiments showed that diffraction gets notably weaker when the DMF concentration is at 40% and above. Diffraction was nearly eliminated at 60% and the crystal dissolved at 70%.

For the DMF experiments, crystals of 8397+1 were transferred to a glass depression plate containing one of the following DMF soak solutions. For the 20% structure the soak solution was 20% (v/v) DMF (Aldrich, HPLC grade), 17% (w/v) PEG 3400, 100 mM sodium citrate (pH 5.6). For the 35% structure the soak solution was 35% (v/v) DMF, 17% (w/v) PEG 3400, 100 mM sodium acetate (pH 4.6). For the 50% structure the soak solution was 50% (v/v) DMF, 17% (w/v) PEG 3400, 100 mM sodium acetate (pH 4.6). All water had been removed from the DMF by storing it over 4 Å, 1/8 in., 4-8 mesh molecular sieves. The plate was then sealed inside a sandwich box that had a 10 mL reservoir of the soak solution. The crystals were soaked in the DMF solution for 14 days before being mounted in quartz capillary tubes for room temperature data collection.

X-ray data collection

X-ray data were measured to a nominal resolution of 1.8 Å for all four DMF conditions (0, 20, 35, and 50%) using a Molecular Structure Corporation (The Woodlands, Texas) four-circle diffractometer with a rotating anode X-ray source (Rigaku) operating at 50 kV and 150 mA. Cu Kα radiation was monochromatized using a graphite crystal. Individual background measurements were made for all reflections. Data from different crystals were merged together using a set of 265 common reflections, which were measured for each crystal as previously described (Monahan et al., 1967). This common block of reflections was collected at the beginning and at the end of data collection. A radiation damage correction (Fletterick et al., 1976) was applied as a function of both time and resolution using these reflections. The DMF data were scaled to the aqueous data set using a single overall scale factor. Programs for data reduction were written in the author's laboratory.

Structure refinement

The starting point for the refinement of all four structures was the high-resolution structure of subtilisin 8350 reported by Pantoliano et al. (1989). All of the water molecules and calcium ions were removed from this structure prior to refinement. All four structures were independently refined from the starting model using X-PLOR (Brünger et al., 1987). Simulated annealing was done in a single round where the structure was heated to 3000 K and cooled in

increments of 25 K. After each cooling step, 50 steps of molecular dynamics simulation were performed. The time step for each of these runs was 0.5 fs. Conventional positional and *B*-factor refinement followed the simulated annealing refinement. For positional refinement, reflections with $F > 2.0\sigma(F)$ and within the resolution range 17.0–1.8 Å were used. For *B*-factor refinement, reflections with $F > 2.0\sigma(F)$ and within the resolution range 5.0–1.8 Å were used. The final *R*-factor was calculated using the 5.0–1.8 Å data shell. Water molecules were located using $2F_o - F_c$ maps with a contour level of 1.2σ. Electron density peaks sometimes appeared in the $2F_o - F_c$ maps as possible water molecules, but did not reappear in the same position or at all after water had been added to the structure. All such waters were deleted. Only waters that reappeared after further refinement and had temperature factors less than 60 Å^2 were retained in the final model.

Initially, calcium ions were modeled as water molecules. However, during intermediate steps of the refinement, the electron densities increased at these sites and the temperature factors decreased to 2 Å^2, the lower limit set in X-PLOR. These observations indicated that a more electron-rich ion was present at these sites. Our confidence in these calcium positions stemmed from the fact that calcium has been detected at these sites in structures reported previously (Pantoliano et al., 1988). Calcium ions were built into sites A and B in the 8397+1 maps. During subsequent refinement rounds, the densities remained large and at 1.2σ were continuous with several carbonyl oxygens, again strengthening our confidence that these were calcium ions.

To provide an unbiased structural model of the region around the catalytic histidine in the native and 50% DMF structures, simulated annealing omit maps were calculated using XPLOR (Hodel et al., 1992). Residues in a 5 Å sphere centered at the Cγ of His64 were omitted from the model. Atoms in a 3 Å shell from 5 to 8 Å were harmonically restrained to prevent them from migrating into the omitted sphere. Simulated annealing was performed with an initial temperature of 1600 K with cooling in 50 K increments until a final temperature of 300 K was obtained. The $2F_o - F_c$ maps for the active sites of the 0, 20, and 35% DMF structures were similar to each other with strong density for the nitrogens of the His64 imidazole. However, the density for the 50% structure was dissimilar. In the native structure (Fig. 3A), there is stronger density for the imidazole Nϵ and weaker density for the Cδ atom. The density for the other two atoms is much weaker, although there is a slight bulge at the Nϵ position. The omit map for the 50% structure is quite different (Fig. 3B). There is a very large bulge in density for Nδ (in the rotated conformation) that would not be as prominent if there was a carbon atom at this location. There is also a large bulge near the rotated Nϵ position. Simulated annealing omit maps were also calculated for the 20 and 35% DMF structures (not shown). They were very similar to the omit map of the native structure.

NMR experiments

For the low pH experiment, subtilisin 8397+1 was dissolved in 20 mM pyridinium-HCl buffer (pH 5). The experiment with the transition state analog was done in 10 mM Tris-HCl buffer (pH 7.5) with 5 mM Boc-Ala-Val-Phe-trifluoromethylketone (TMFK). We verified that TMFK completely inhibited subtilisin in 50% DMF at concentrations well below the millimolar range used in the NMR experiment. These solutions were then diluted with an equal volume of either water or DMF to give a final subtilisin concentration of 1.5 mM. The final solutions were cooled to 1 °C where the spectra were collected. There is a substantial heat of mixing for DMF/water solutions, so the DMF was added dropwise with rapid mixing and cooling after each addition. The pH of these final cooled solutions were measured with a Ag/AgCl electrode calibrated at 1 °C. The pyridinium-HCl and pyridinium-HCl/DMF samples had an apparent pH of 5.8 and 5.7, respectively, while the Tris-HCl and Tris-HCl/DMF samples both had an apparent pH of 7.5.

Acknowledgments

We thank Lori C. Zeringue for her initial refinement results of new structures of subtilisin in DMF. We thank Neela H. Yennawar and Hemant P. Yennawar for helpful discussions and technical advice. This work was supported by grants from the Office of Naval Research (G.K.F. and C.-H.W.) and the NIH (G.K.F.).

References

Abrahmsen L, Tom J, Burnier J, Butcher KA, Kossiakoff A, Wells JA. 1991. Engineering subtilisin and its substrates for efficient ligation of peptide bonds in aqueous solution. *Biochemistry 30*:4151–4159.

Ash EL, Sudmeier JL, DeFabo EC, Bachovchin WW. 1997. A low-barrier hydrogen bond in the catalytic triad of serine proteases? Theory versus experiment. *Science 278*:1128–1132.

Bachovchin WW, Roberts JD. 1978. Nitrogen-15 nuclear magnetic resonance spectroscopy. The state of histidine in the catalytic triad of alpha-lytic protease. Implications for the charge-relay mechanism of peptide bond cleavage by serine proteases. *J Am Chem Soc 100*:8041–8047.

Brünger AT, Kuriyan J, Karplus M. 1987. Crystallographic R factor refinement by molecular dynamics. *Science 235*:458–460.

Byers LD, Koshland DE Jr. 1978. On the mechanism of action of methyl chymotrypsin. *Bioorg Chem 7*:15–33.

Carter P, Wells JA. 1987. Engineering enzyme specificity by "substrate-assisted catalysis." *Science 237*:394–399.

Fersht AR, Renard M. 1974. pH dependence of chymotrypsin catalysis. *Biochemistry 13*:1416–1426.

Fletterick RJ, Sygusch J, Murray N, Madsen NB, Johnson LN. 1976. Low-resolution structure of the glycogen phosphorylase a monomer and comparison with phosphorylase b. *J Mol Biol 103*:1–13.

Frey PA, Whitt SA, Tobin JB. 1994. A low-barrier hydrogen bond in the catalytic triad of serine proteases. *Science 264*:1927–1930.

Gololobov MY, Voyushina TL, Stepanov VM, Adlercreutz P. 1992. Organic solvent changes the chymotrypsin specificity with respect to nucleophiles. *FEBS Lett 307*:309–312.

Halkides CJ, Wu YQ, Murray CJ. 1996. A low-barrier hydrogen bond in subtilisin: 1H and 15N NMR studies with peptidyl trifluoromethyl ketones. *Biochemistry 35*:15941–15948.

Henderson R. 1971. Catalytic activity of alpha-chymotrypsin in which histidine 57 has been methylated. *Biochem J 124*:13–18.

Hodel A, Kim S-H, Brünger AT. 1992. Model bias in macromolecular crystal structures. *Acta Crystallogr A 48*:851–858.

Homandberg GA, Mattis JA, Laskowski M Jr. 1978. Synthesis of peptide bonds by proteinases. Addition of organic cosolvents shifts peptide bond equilibria toward synthesis. *Biochemistry 17*:5220–5227.

Jones TA, Zou JY, Cowan SW, Kjeldgaard M. 1991. Improved methods for binding protein models in electron density maps and the location of errors in these models. *Acta Crystallogr A 47*:110–119.

Kidd RD, Yennawar HP, Sears P, Wong C-H, Farber GK. 1996. A weak calcium binding site in subtilisin BPN′ has a dramatic effect on protein stability. *J Am Chem Soc 118*:1645–1650.

Kuhl P, Halling PJ, Jakubke H-D. 1990. Chymotrypsin suspended in organic solvents with salt hydrates is a good catalyst for peptide synthesis from mainly undissolved reactants. *Tetrahedron Lett 31*:5213–5216.

Markley JL. 1978. Hydrogen bonds in serine proteinases and their complexes with protein proteinase inhibitors. Proton nuclear magnetic resonance studies. *Biochemistry 17*:4648–4656.

Markley JL, Ibañez IB. 1978. Zymogen activation in serine proteases. Proton magnetic resonance pH titration studies of the two histidines of bovine chymotrypsinogen A and chymotrypsin A_α. *Biochemistry 17*:4627–4640.

Monahan JE, Schiffer M, Schiffer JP. 1967. On the scaling of X-ray photographs. *Acta Crystallogr 22*:322.

Pantoliano MW, Whitlow M, Wood JF, Dodd SW, Hardman KD, Rollence ML, Bryan PN. 1989. Large increases in general stability for subtilisin BPN′ through incremental changes in the free energy of unfolding. *Biochemistry 28*:7205–7213.

Pantoliano MW, Whitlow M, Wood JF, Rollence ML, Finzel BC, Gilliland GL, Poulos TL, Bryan PN. 1988. The engineering of binding affinity at metal ion binding sites for the stabilization of proteins: Subtilisin as a test case. *Biochemistry 27*:8311–8317.

Petsko GA. 1985. Diffraction methods for biological macromolecules. Flow cell construction and use. *Methods Enzymol 114*:141–146.

Sears P, Schuster M, Wang P, Witte K, Wong C-H. 1994. Engineering subtilisin for peptide coupling: Studies on the effects of counterions and site-specific modifications on the stability and specificity of the enzyme. *J Am Chem Soc 116*:6521–6530.

Stahl M, Mansson MO, Mosbach K. 1990. The synthesis of a D-amino acid ester in an organic media with alpha-chymotrypsin modified by a bio-imprinting procedure. *Biotechnol Lett 12*:161–166.

Tawaki S, Klibanov AM. 1992. Inversion of enzyme enantioselectivity mediated by the solvent. *J Am Chem Soc 114*:1882–1884.

Tobin JB, Whitt SA, Cassidy CS, Frey PA. 1995. Low-barrier hydrogen bonding in molecular complexes analogous to histidine and aspartate in the catalytic triad of serine proteases. *Biochemistry 34*:6919–6924.

Wells JA, Estell DA. 1988. Subtilisin—An enzyme designed to be engineered. *TIBS 13*:291–297.

West JB, Hennen WJ, Lalonde JL, Bibbs JA, Zhong Z, Meyer EF Jr, Wong C-H. 1990. Enzymes as synthetic catalysts, mechanistic and active-site considerations of natural and modified chymotrypsin. *J Am Chem Soc 112*:5313–5320.

Wong C-H. 1989. Enzymatic catalysts in organic synthesis. *Science 244*:1145–1152.

Wong C-H, Chen ST, Hennen WJ, Bibbs JA, Wang Y-F, Liu JL-C, Pantoliano MW, Whitlow M, Bryan PN. 1990. Enzymes in organic synthesis, use of subtilisin and a highly stable mutant derived from multiple site-specific mutations. *J Am Chem Soc 112*:945–953.

Zaks A, Klibanov AM. 1985. Enzyme-catalyzed processes in organic solvents. *Proc Natl Acad Sci USA 82*:3192–3196.

Zaks A, Klibanov AM. 1986. Substrate specificity of enzymes in organic solvents vs. water is reversed. *J Am Chem Soc 108*:2767–2768.

Zaks A, Klibanov AM. 1988. Enzymatic catalysis in nonaqueous solvents. *J Biol Chem 263*:3194–3201.

Zhong Z, Bibbs JA, Yuan W, Wong C-H. 1991a. Engineering subtilisin for reaction in dimethylformamide. *J Am Chem Soc 113*:683–684.

Zhong Z, Bibbs JA, Yuan W, Wong C-H. 1991b. Active-site-directed modification of subtilisin. *J Am Chem Soc 113*:2259–2263.